



AFRL-OSR-VA-TR-2013-0617

**EXPERIMENTAL STUDY OF THE STRUCTURE-PROPERTY
RELATIONSHIP OF MOLECULAR JUNCTIONS**

PRAMOD REDDY

UNIV OF MICHIGAN

**12/11/2013
Final Report**

DISTRIBUTION A: Distribution approved for public release.

**AIR FORCE RESEARCH LABORATORY
AF OFFICE OF SCIENTIFIC RESEARCH (AFOSR)/RSA
ARLINGTON, VIRGINIA 22203
AIR FORCE MATERIEL COMMAND**

| | | | | | |
|---|--------------------|-----------------------|-----------------------------------|--|--|
| REPORT DOCUMENTATION PAGE | | | | <i>Form Approved</i> OMB No. 0704-0188 | |
| Public reporting burden for this collection of information is estimated to average 1 hour per response, including the time for reviewing instructions, searching existing data sources, gathering and maintaining the data needed, and completing and reviewing this collection of information. Send comments regarding this burden estimate or any other aspect of this collection of information, including suggestions for reducing this burden to Department of Defense, Washington Headquarters Services, Directorate for Information Operations and Reports (0704-0188), 1215 Jefferson Davis Highway, Suite 1204, Arlington, VA 22202-4302. Respondents should be aware that notwithstanding any other provision of law, no person shall be subject to any penalty for failing to comply with a collection of information if it does not display a currently valid OMB control number. PLEASE DO NOT RETURN YOUR FORM TO THE ABOVE ADDRESS. | | | | | |
| 1. REPORT DATE (DD-MM-YYYY) | | 2. REPORT TYPE | | 3. DATES COVERED (From - To) | |
| 4. TITLE AND SUBTITLE | | | | 5a. CONTRACT NUMBER | |
| | | | | 5b. GRANT NUMBER | |
| | | | | 5c. PROGRAM ELEMENT NUMBER | |
| 6. AUTHOR(S) | | | | 5d. PROJECT NUMBER | |
| | | | | 5e. TASK NUMBER | |
| | | | | 5f. WORK UNIT NUMBER | |
| 7. PERFORMING ORGANIZATION NAME(S) AND ADDRESS(ES) | | | | 8. PERFORMING ORGANIZATION REPORT NUMBER | |
| 9. SPONSORING / MONITORING AGENCY NAME(S) AND ADDRESS(ES) | | | | 10. SPONSOR/MONITOR'S ACRONYM(S) | |
| | | | | 11. SPONSOR/MONITOR'S REPORT NUMBER(S) | |
| 12. DISTRIBUTION / AVAILABILITY STATEMENT | | | | | |
| 13. SUPPLEMENTARY NOTES | | | | | |
| 14. ABSTRACT | | | | | |
| 15. SUBJECT TERMS | | | | | |
| 16. SECURITY CLASSIFICATION OF: | | | 17. LIMITATION OF ABSTRACT | 18. NUMBER OF PAGES | 19a. NAME OF RESPONSIBLE PERSON |
| a. REPORT | b. ABSTRACT | c. THIS PAGE | | | 19b. TELEPHONE NUMBER (include area code) |

FINAL REPORT

EXPERIMENTAL STUDY OF THE STRUCTURE-PROPERTY RELATIONSHIP OF MOLECULAR JUNCTIONS

Institution Name & Address:

The Regents of the University of Michigan,
3003 S. State Street,
Room 1056, Ann Arbor
MI 48109-1274

Principal Investigator:

Pramod Sangi Reddy
Department of Mechanical Engineering
University of Michigan, Ann Arbor, 48109
Tel: 734-615-5952, Fax: 734-647-3170
Email: pramodr@umich.edu

Program Manager:

Dr. Ali Sayir
Aerospace Materials for Extreme Environments
Air Force Office of Scientific Research
Email: ali.sayir@afosr.af.mil

ABSTRACT: In this work we have developed novel experimental platforms to understand the structure property relationship of molecular junctions. Specifically, we sought to investigate the feasibility of creation of organic-based thermoelectric energy conversion. Towards this goal, we first developed a picowatt-resolution calorimeter that is critical for characterizing thermal transport through molecular junctions (**Sadat *et al.*, Appl. Phys. Lett., 2011**). Subsequently, we developed a novel thermal imaging tool for probing temperature fields with nanoscale resolution (**Kim *et al.*, ACS Nano, 2012**). Finally, we used the novel scanning thermal imaging techniques (**Jeong *et al.*, In Review, ACS Nano**) to both understand Joule heating in nanoscale interconnects and to establish temperature differentials across nanoscale gaps. These three terminal devices were created to tune the electronic structure of molecular junctions while probing their thermoelectric properties. We have recently used these devices to tune thermoelectric effects in molecular junctions and preparing these interesting results for review and publication (**To be submitted to Nature Nanotechnology**).

Key Words: Thermoelectrics, Nanofabrication, Organic Molecules.

The goal of this project was to understand the thermoelectric properties of molecular junctions. Specifically, we sought to understand the relationship between thermoelectric properties and the electronic structure of molecular junctions with the goal of creating efficient organic based thermoelectric materials. To accomplish this goal we adopted a multipronged approach. First, we sought to develop the capabilities to perform three terminal thermoelectric measurements of molecular junctions by fabricating a molecular field effect transistor with a gate electrode that is in close proximity (a few nanometers) of the molecule. In order to accomplish these measurements it was necessary to establish temperature differentials of ~ 1 K across metal electrodes separated by ~ 1 nanometer. Towards this goal we extensively leveraged our nanofabrication capabilities and developed novel thermometry and calorimetric tools developed by us recently. In this report we first describe the novel scanning probe techniques developed as part of this project and provide details of the techniques used in fabricating the probes. Subsequently, we will describe the novel three terminal devices required for the measurements and also elaborate on how we fabricated the devices and characterized the temperature differentials in them. We also present unpublished results that show how we have leveraged these nanoscale devices to elucidate the relationship between electronic structure and thermoelectric properties of molecular junctions as well as to understand the role of Joule heating in the electromigration of devices. Finally, we also present details of the picowatt resolution calorimeter developed by us which is critical for extending the current studies into the thermal domain.

1. Ultra-high vacuum Scanning Thermal Microscopy

Probing temperature fields with nanoscale resolution is critical for accomplishing the goals of this project. Although impressive progress had been achieved in scanning thermal microscopy (SThM) [1-7], obtaining quantitative information regarding thermal fields using SThM has remained elusive. Further, achieving high spatial resolutions of ~ 10 nm or lower had not been possible despite the need for such resolution in detailed thermal studies on nano-scale devices. These apparent limitations of SThM were due to operation in ambient conditions where local measurement of temperature fields is impeded by parasitic heat transfer between the tip and the sample via conduction through both air and the liquid meniscus that exists at the tip-sample interface[8]. Further, the spatial resolution of SThM in the ambient was limited to ~ 50 nm due to the large tip-sample contact size (~ 50 nm) that arises from the liquid film existing at the tip-sample interface[8].

As part of this project we have recently developed an ultra-high vacuum (UHV)-based scanning thermal microscope (SThM) technique that **overcomes all these challenges**. [9] In this technique (Figure 1), a custom fabricated atomic force microscope (AFM)

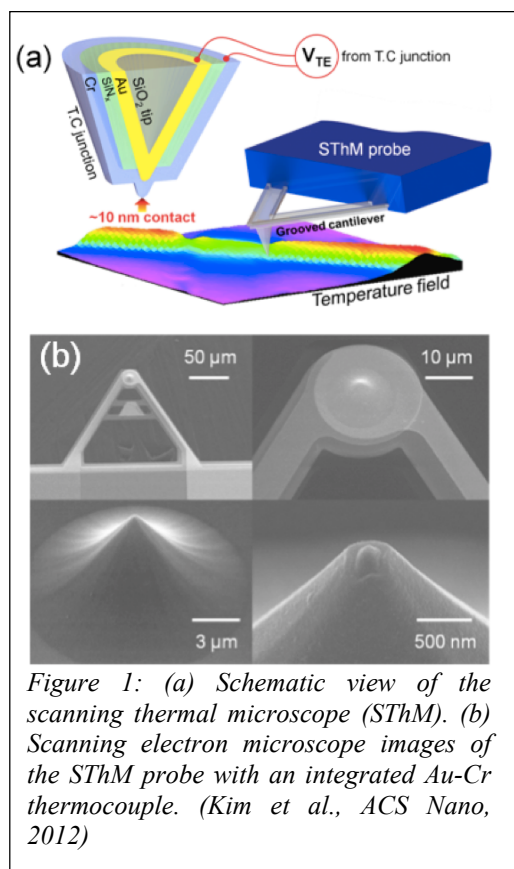


Figure 1: (a) Schematic view of the scanning thermal microscope (SThM). (b) Scanning electron microscope images of the SThM probe with an integrated Au-Cr thermocouple. (Kim et al., ACS Nano, 2012)

cantilever with a nanoscale Au-Cr thermocouple integrated into the tip of the probe is used to measure temperature fields of surfaces. Operation in an UHV environment eliminates parasitic heat transport between the tip and the sample enabling quantitative measurement of temperature fields on metal and dielectric surfaces with nanoscale resolution.

The capabilities of UHV-SThM can be seen from the thermal image (Figure 2) of a 200 nm wide and 50 nm thick Platinum (Pt) line, which was heated by passing a small electrical current. The thermal image (Figure 2b) corresponds to a region where the 200 nm wide Pt line (through which an electrical current is flowing) is connected to a 1 μm wide Pt line (probe lead through which no electrical current is passing, see Figure 2a). As can be seen from the figure, the temperature decays rapidly along the 1 μm wide line as the Pt line acts as a fin. This clearly demonstrates that thermal fields can be imaged with nanoscale resolution using the UHV-SThM technique. More detailed studies[9], performed by us, unambiguously demonstrate that UHV-SThM *is capable of quantitatively mapping temperature fields with ~ 15 mK temperature resolution and ~ 10 nm spatial resolution.*

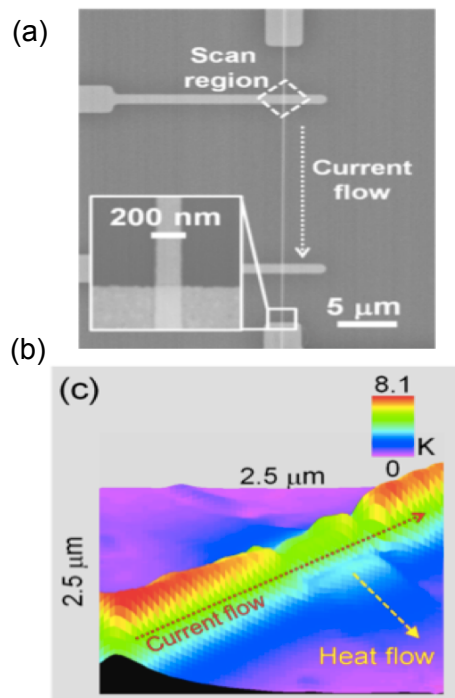
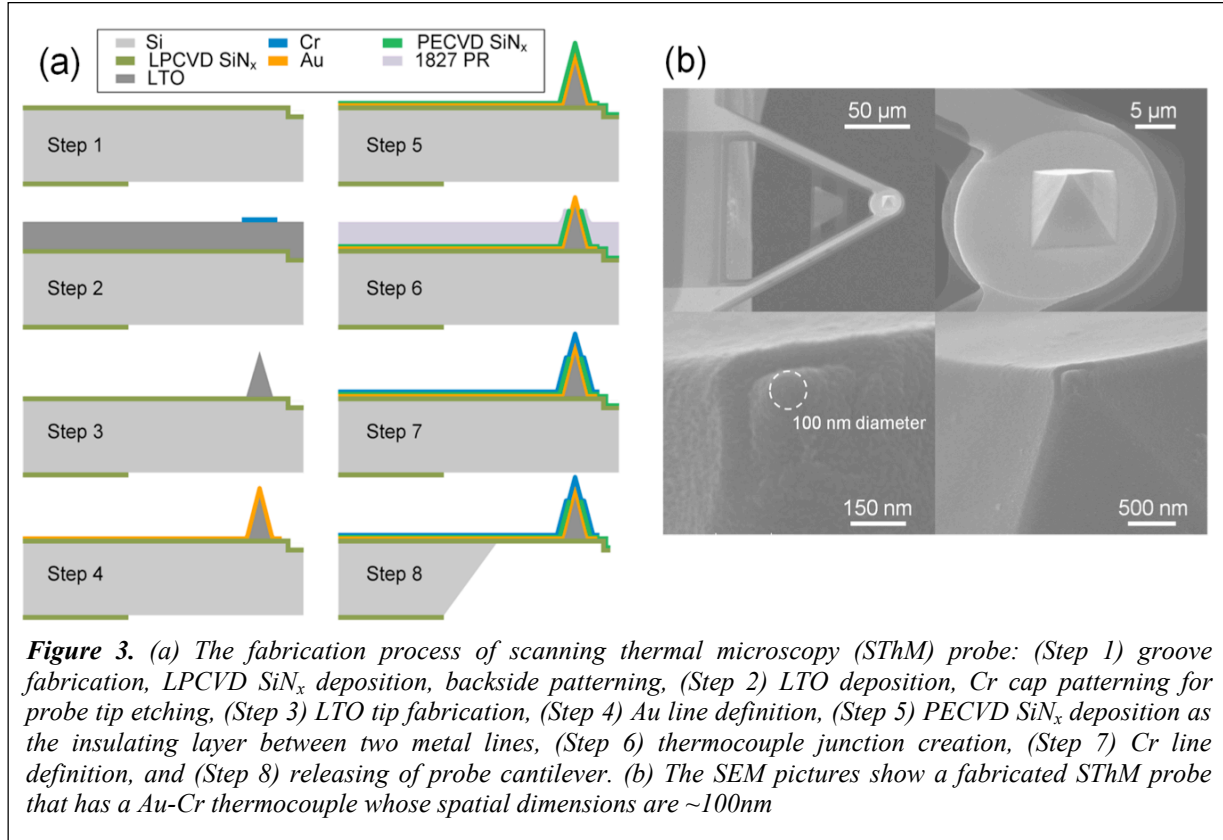


Figure 2: (a) SEM image of a 200 nm wide Pt line. (b) shows a thermal image in a $2.5 \mu\text{m} \times 2.5 \mu\text{m}$ region where the 200 nm wide Pt line lies on top of a 1 μm wide Pt line. (Kim et al., ACS Nano, 2012)

Fabrication of SThM Probes: The steps involved in the fabrication of the scanning thermal microscopy (SThM) probes are shown in Fig. 3 and are as follows: (Step1) The fabrication process of SThM probe starts by lithographically making a 1.6 μm deep groove on a double side polished silicon (Si) wafer by a plasma etch. We note that this groove increases the stiffness of probe cantilever and prevents large deflections of the cantilever due to laser heating in ultra high vacuum (UHV) conditions: such deflections are expected due to differences in the thermal expansion coefficients of the materials of which the cantilever is made (more details of the effect of differential thermal expansion are provided later in the SI). Subsequently, 500 nm thick low-stress low pressure chemical vapor deposition (LPCVD) silicon nitride (SiN_x) is deposited on both sides of the wafer. Then, the back side of the wafer is lithographically patterned by plasma etching to facilitate the cantilever release process in the final step of the fabrication. (Step 2) 8 μm thick low temperature silicon oxide (LTO) is deposited on both sides of the wafer and is annealed at 1000°C for 1 hour in order to reduce the residual stress of low-stress nitride and LTO layers: this LTO layer will eventually be patterned to create the probe tip. Subsequently, a Cr cap (150 nm thick) is lithographically patterned by Cr etching and is designed to facilitate the etching of LTO to create the probe tip. (Step 3) The LTO probe tip is fabricated by buffered HF ($\text{HF} : \text{NH}_4\text{F} = 1:5$) etching, which takes ~ 100 minutes. In order to obtain a sharp tip the etching status of the tip is monitored, at 10 minute intervals, by using an optical microscope. (Step 4) After fabrication of a sharp LTO tip, a gold (Au) line (Cr/Au: 5/90 nm) is lithographically defined by sputtering and Au etching. This Au line is the first metal layer of the SThM probe. (Step 5) The insulating layer between two metal lines is created by depositing 70 nm of SiN_x on the probe by

plasma enhanced chemical vapor deposition (PECVD). (Step 6) In order to create a nanoscale thermocouple junction on the apex of the probe tip, a 6 μm thick Shipley Microposit S1827 photoresist is deposited on the probe. The photoresist and PECVD SiN_x is slowly plasma etched until a very small portion of the Au layer is extruded. (Step 7) A Chromium (Cr) line (Cr: 90 nm) is lithographically defined by sputtering and Cr etching. This Cr line is the second metal layer of the SThM probe, and is deposited to create a nanoscale Au-Cr thermocouple junction at the end of the probe tip. (Step 8) Finally, the SThM probe is released by KOH etching.

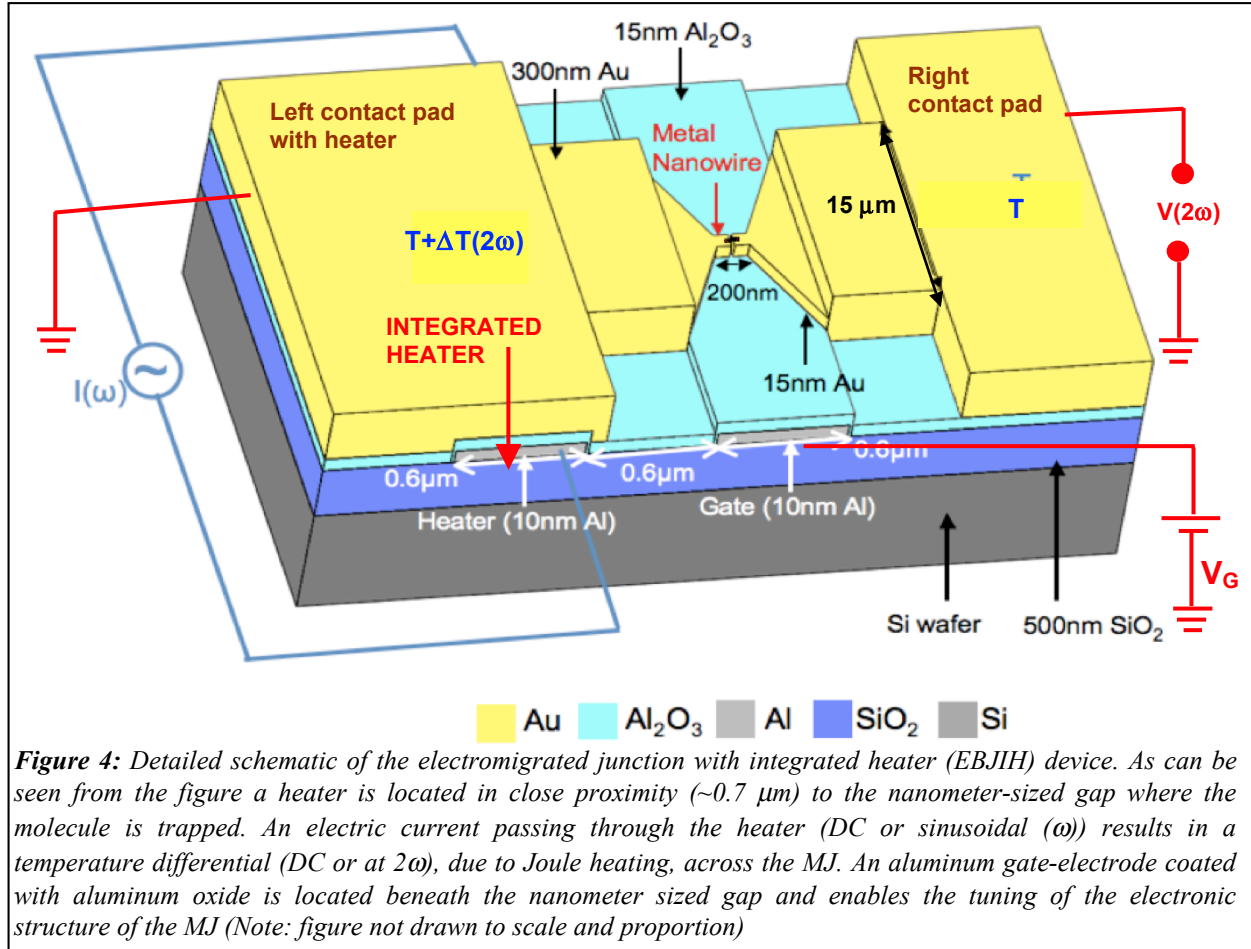


2. Creation of Three Terminal Devices and Characterization of Temperature Differentials

A new approach is required to study the relation between electronic structure and thermoelectric properties of MJs because none of the existing techniques are capable of performing these difficult measurements. In order to accomplish this task, we developed a novel technique that involves the creation of an electromigrated break junction device with an integrated heater (EBJIH). The details of this approach are presented next.

Description of Three Terminal Devices: The devices that we fabricated in this project are conceptually simple. Here, we first provide a general overview of the EBJIH device and subsequently describe the devices that we have actually fabricated. The EBJIH device consists of a metal nanowire that is in contact with two large contact pads (Fig. 4): this metal nanowire is used to create a molecular junction (MJ) by employing an electromigration procedure described elsewhere. Further, an aluminum (Al) gate electrode covered with a thin layer of aluminum oxide (Al_2O_3) is also located below the metal nanowire as shown in Fig. 4. This gate electrode can be used to tune the electronic structure of MJs. In addition to these features, an electrical heater is

also integrated into the device and is located in close proximity to the region where a nanometer-sized gap will be created to trap a single molecule (Fig. 4). A temperature differential of approximately a few Kelvin can be created across the nanometer-sized MJ by supplying an electrical current through the heater (a sinusoidal current can also be supplied to cause an oscillation in the temperature differential across the MJ). While the existence of such large temperature differentials across a nanometer-sized gap may seem surprising, a careful computational analysis of the temperature field in the device strongly supports this claim and is validated by our experiments (discussed later). The thermoelectric voltage differential across the molecular junction for known temperature differentials can be measured directly while applying



a gate voltage to study the effect of electronic structure of a MJ on its thermoelectric properties.

Thermal Modeling (Unpublished Results): The proposed device (Fig. 4) consists of a metallic (gold) nanowire that is $\sim 15 \text{ nm}$ thick is connected to two large contact pads as shown in the figure. The Au nanowire is located above an Al gate electrode that is coated with $\sim 15 \text{ nm}$ thick aluminum oxide layer (this thickness is larger than that used in the EBJ devices described in an earlier section, the reason for this increased thickness is explained in detail later). An Aluminum heater line that is $\sim 10 \text{ nm}$ thick and $\sim 0.6 \mu\text{m}$ wide is located under the left contact pad and is electrically isolated from the left contact pad by an $\sim 15 \text{ nm}$ thick aluminum oxide layer. A MJ, where a single molecule is trapped in a nanometer sized gap in the metal nanowire, can be

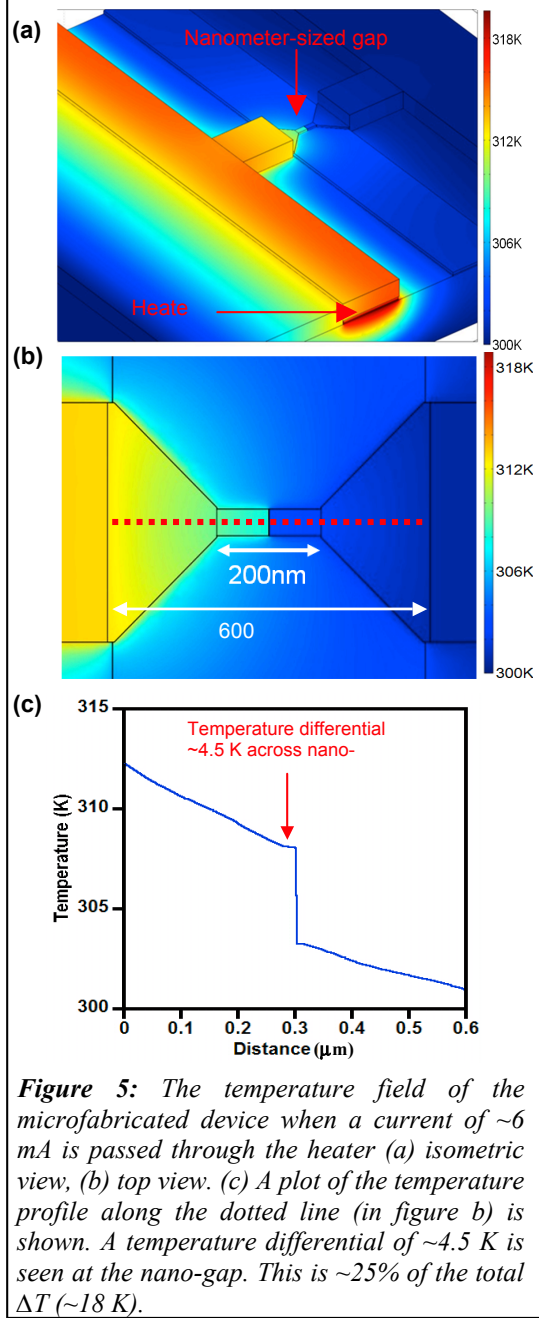


Figure 5: The temperature field of the microfabricated device when a current of ~ 6 mA is passed through the heater (a) isometric view, (b) top view. (c) A plot of the temperature profile along the dotted line (in figure b) is shown. A temperature differential of ~ 4.5 K is seen at the nano-gap. This is $\sim 25\%$ of the total ΔT (~ 18 K).

created by following the electromigration procedure described in the previous section. If a DC electric current ($\omega = 0$) is supplied through the heater line, as shown in Fig. 9, it would cause an increase in the temperature of the heater line and lead to a thermal gradient along the metal nanowire: the region in the left electrode immediately above the heater line would be at a higher temperature, $T + \Delta T$, whereas the right electrode which is far away from the heater will be at a lower temperature T . An important question in this context is: what fraction of the temperature differential (ΔT) drops across the nanoscale gap? In order to answer this question, we calculated the temperature field in the device, for a range of electrical currents, using a commercially available finite element software (COMSOL) (*Note: In these calculations, care was taken to account for the reduction in the thermal conductivity of thin films due to the increased boundary scattering of electrons and phonons*). The result for one representative choice of current (~ 6 mA) is shown in Fig. 5.

These modeling results unambiguously show that $\sim 25\%$ of the applied temperature differential, ΔT , drops across the nanometer-sized junction (Fig. 5c). This temperature differential arises due to a large mismatch in the thermal conductivities of gold (~ 150 W/m \cdot K [10]) and aluminum oxide (< 1 W/m \cdot K [11]) thin films. This large mismatch suggests that a large temperature differential could arise across the nanometer-sized gap as heat has to flow from the left electrode to the right electrode through the oxide layer, which has a low thermal conductivity. In fact, the thickness of the Al_2O_3 layer is purposefully chosen to be thicker ~ 15 nm as opposed to ~ 5 nm thickness used in previous EBJs[12] as this increases

the thermal isolation across the nanometer-sized gap. In this qualitative argument, the flow of heat through the molecule bridging the two electrodes is neglected as the thermal resistance of a molecule is expected to be extremely large ($\sim 10^{11}$ K/W)[13-16]. The above discussion strongly suggests that it is indeed possible to establish temperature differentials across a MJ that is created using an EBJ technique. Later, we will describe how these temperature differentials are characterized experimentally and confirm that they are indeed in reasonable correspondence with computational predictions.

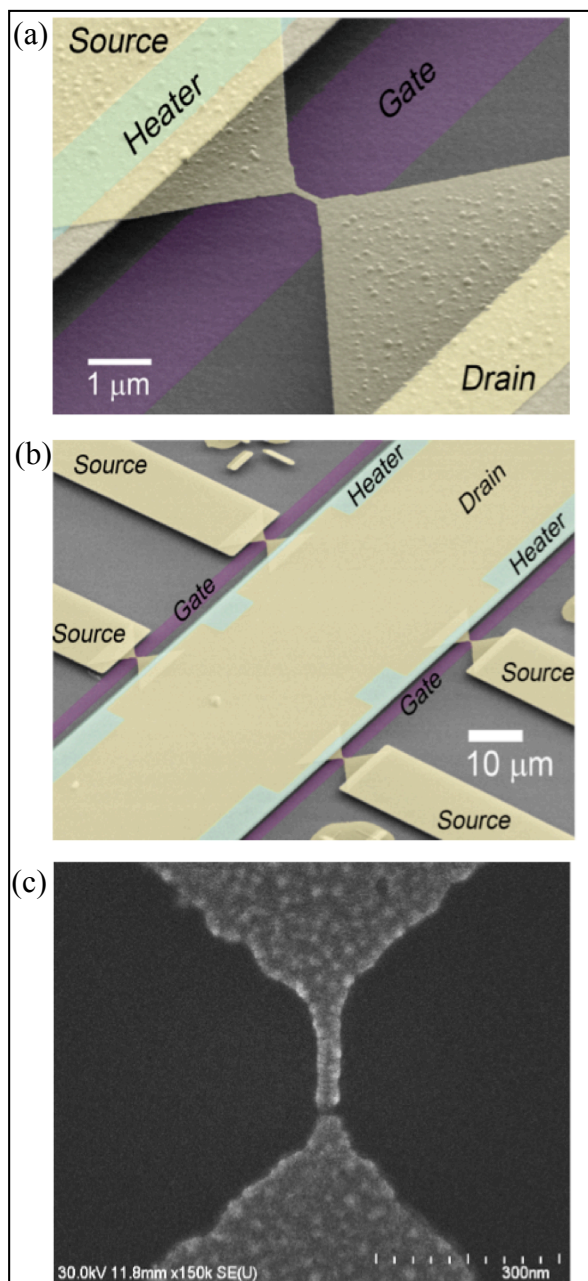


Figure 6: (a & b) Scanning electron micrograph images of the nanofabricated EBJIH devices. False coloring used to highlight the gate and heater electrodes. (c) SEM image of the electromigrated device. [Unpublished Results]

Fabrication of the Proposed Device:

Fabrication of the proposed device is readily possible using the resources available in the nanofabrication facility at the University of Michigan. In Fig. 6 we show scanning electron micrograph (SEM) images of the fabricated devices (a & b). The location of the gate and heater electrodes is shown via a false coloring scheme. We also show an SEM image of a device that has been electromigrated to create a nanoscale gap (Fig. 6c).

Nanoscale Thermal Imaging to Experimentally Determine the Temperature Field:

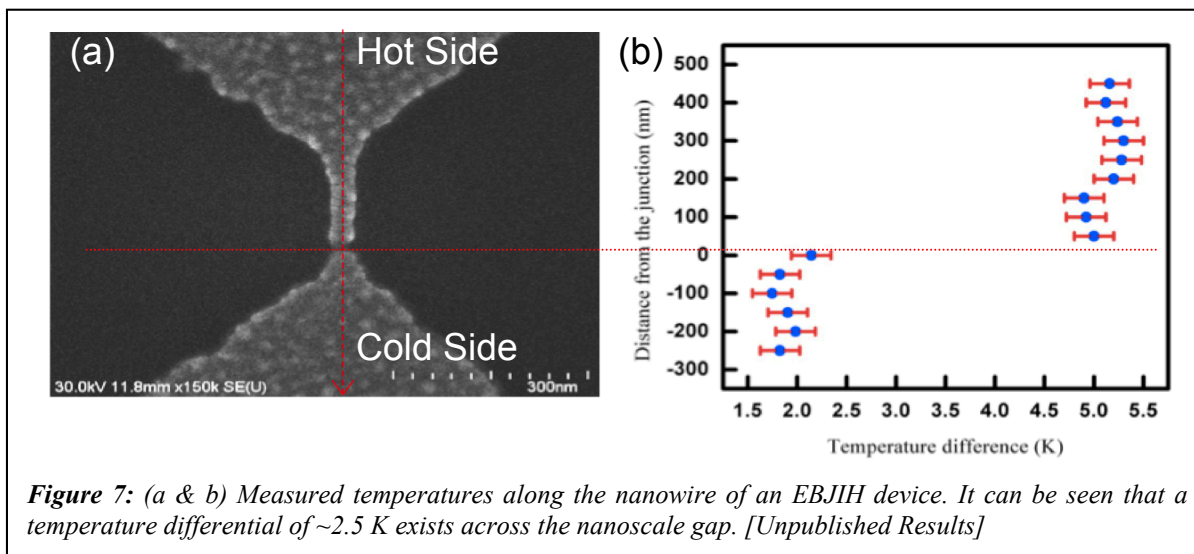
In order to experimentally characterize the temperature fields in the EBJIH devices, we employed the UHV-SThM technique that we developed as part of this project. The measured temperature fields shown in Fig. 7 unambiguously show that a large temperature differential exists in the nanoscale gap of the device confirming the feasibility of establishing temperature differential across nanoscale gaps.

Molecular Gating Measurements

(Unpublished Results): The EBJIH device, described above is currently being employed by us to tune electronic structure and probe the thermoelectric properties of molecular junctions. Our recent results indicate that it is indeed possible to tune the thermoelectric properties of molecular junctions. These results are currently being analyzed and are being submitted for review and publication in *Nature Nanotechnology*.

Summary: We have now successfully fabricated the devices necessary to probe thermoelectric effect in molecular junctions. We have already characterized temperature fields in these devices

and are now performing three terminal measurements of thermoelectric properties of molecular junctions. We are currently analyzing the obtained results and performing additional experiments to conclusively determine the relationship between the electronic structure and thermoelectric properties. We are hoping to report these important results in a top scientific journal.



3. Nanoscale Thermal Imaging to Understand Electromigration in Nanowires

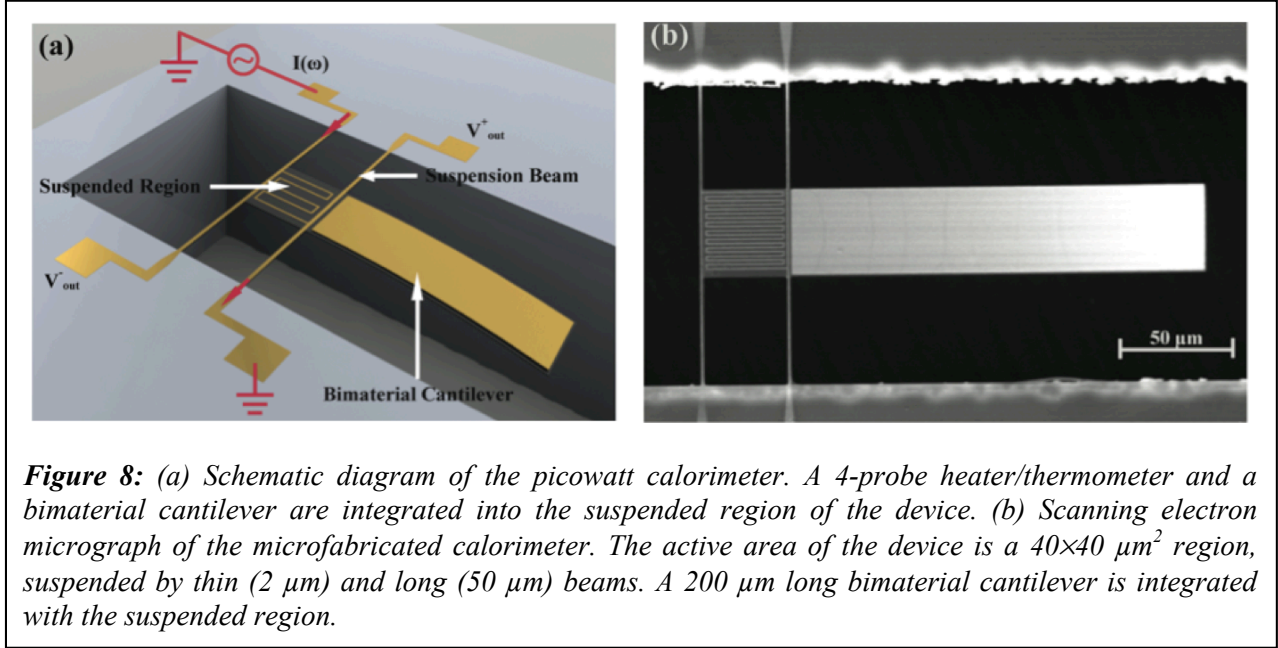
Understanding heat dissipation (Joule heating) and transport in nanoscale devices is critical for realizing novel nanoscale functional devices. In fact, Joule heating is widely expected to play an important role in electromigration induced device failure: a process where atoms in a device are displaced due to momentum transfer between charge carriers and the lattice. Electromigration in devices is always accompanied by Joule heating, which accelerates the electromigration process by affecting the mobility of atoms and is well known to limit the operating voltages and the reliability of functional devices. To better understand the role of Joule heating on electromigration several research groups have indirectly estimated the local temperature changes during electromigration. However, a direct quantification of temperature fields during electromigration—with nanoscale resolution—has remained elusive although such knowledge is critical for both increasing the reliability of nanoscale devices and creating functional devices that take advantage of electromigration.

In this work, we leveraged the advances in ultra-high vacuum scanning thermal microscopy (UHV-SThM) accomplished in this project that enable quantitative nanoscale measurements of temperature fields. Using this technique, we probed temperature fields in prototypical bow-tie shaped gold (Au) devices (see Fig. 6). Our results unambiguously illustrate that electromigration begins at temperatures significantly lower than the melting temperature of gold. Further, we show that during electromigration voids predominantly accumulate at the cathode resulting in both local hot spots and asymmetric temperature distributions. These results provide novel insights into the microscopic details of hot spot evolution during electromigration and are expected to guide the design of reliable nanoscale functional devices. These results have been recently submitted for review and publication in ACS Nano.






4. Picowatt Resolution Calorimetry

As part of this project we have recently developed a new experimental technique that enables us to perform heat flow calorimetry with <4 picowatt resolution. In order to accomplish this goal, we microfabricated novel devices that feature a bimaterial cantilever temperature sensor

integrated into a micro-island that was suspended by thin and long beams to achieve a low overall thermal conductance of ~ 600 nW/K. By placing the device in a high vacuum environment and taking other precautions we successfully decoupled the device from ambient acoustic and ambient vibrations. This level of isolation enabled us to successfully measure modulated temperature changes, using the bimaterial cantilever, with ~ 6 μ K resolution. Overall, given the low thermal conductance and excellent temperature resolution, we were able to measure heat flows with a resolution < 4 pW (600 nW/K \times 6 μ K). We recently reported these results in *Applied Physics Letters*[17].



Fabrication of Calorimeter: The Fabrication process starts by depositing low-stress LP-CVD nitride on both sides of $500 \mu\text{m}$, p-type Si wafer (Fig. 9). Patterns of sensing, matching and heater coils are transferred onto the photoresist by a combination of high-resolution lithography and electron beam evaporation of 30 nm thick Pt film on the wafers, followed by the lift-off process. All Pt coils are $0.8 \mu\text{m}$ wide at the coil region and $1 \mu\text{m}$ wide on suspension beams. Subsequently, two more lift-off process is used to deposit extra 100 nm of Au on current carrying beams and 300 nm thick electrical leads to wire-bond pads. Next, suspension beam pattern is transferred to nitride layer by patterning photoresist as a soft mask and plasma etching of nitride film. All devices are released at the wafer level, by wet etching process using 40% KOH solution in DI water. Eventually all devices were release using critical point drying technique to prevent stiction between long suspension beams.

| | Process | Detail | Schematic |
|---|---|---------------------------|--|
| 1 | LP-CVD Low-stress silicon nitride deposition on both sides. | Nitride: 500nm |  |
| 2 | Heater line pattern transfer | Cr/Pt: 3/30 nm, lift-off |  |
| 3 | Electrical connection pattern transfer | Cr/Au: 3/100 nm, lift-off |  |
| 4 | Suspended active area pattern transfer on nitride layer | Plasma etch |  |
| 5 | Wet Etch device release. | 40% KOH at 85°C |  |

Silicon: , Low-stress Silicon nitride: , Platinum thermometer: , Electrical connection Au Line: .

Figure 9: (a) The fabrication process of the calorimeter with an integrated bimaterial cantilever temperature sensor.

References:

1. Weaver, J.M.R., L.M. Walpita, and H.K. Wickramasinghe, *Optical-Absorption Microscopy and Spectroscopy with Nanometer Resolution*. Nature, 1989. **342**(6251): p. 783-785.
2. Majumdar, A., *Scanning thermal microscopy*. Annual Review of Materials Science, 1999. **29**: p. 505-585.
3. Christofferson, J. and A. Shakouri, *Thermoreflectance based thermal microscope*. Review of Scientific Instruments, 2005. **76**(2): p. -.
4. Fletcher, D.A., G.S. Kino, and K.E. Goodson, *Thermal microscopy with a microfabricated solid immersion lens*. Microscale Thermophysical Engineering, 2003. **7**(4): p. 267-273.
5. Williams, C.C. and H.K. Wickramasinghe, *Scanning thermal profiler*. Applied Physics Letters, 1986. **49**(23): p. 1587-1589.
6. Kim, K., J. Chung, G. Hwang, O. Kwon, and J.S. Lee, *Quantitative Measurement with Scanning Thermal Microscope by Preventing the Distortion Due to the Heat Transfer through the Air*. ACS Nano, 2011. **5**(11): p. 8700-8709.
7. Sadat, S., A. Tan, Y.J. Chua, and P. Reddy, *Nanoscale Thermometry Using Point Contact Thermocouples*. Nano Letters, 2010. **10**(7): p. 2613-2617.
8. Shi, L. and A. Majumdar, *Thermal transport mechanisms at nanoscale point contacts*. Journal of Heat Transfer-Transactions of the Asme, 2002. **124**(2): p. 329-337.
9. Kim, K., W. Jeong, W. Lee, and P. Reddy, *Ultra-High Vacuum Scanning Thermal Microscopy for Nanometer Resolution Quantitative Thermometry*. ACS Nano, 2012.
10. Chen, G. and P. Hui, *Thermal conductivities of evaporated gold films on silicon and glass*. Applied Physics Letters, 1999. **74**(20): p. 2942-2944.
11. Behkam, B., Y.Z. Yang, and M. Asheghi, *Thermal property measurement of thin aluminum oxide layers for giant magnetoresistive (GMR) head applications*. International Journal of Heat and Mass Transfer, 2005. **48**(10): p. 2023-2031.
12. Liang, W.J., M.P. Shores, M. Bockrath, J.R. Long, and H. Park, *Kondo resonance in a single-molecule transistor*. Nature, 2002. **417**(6890): p. 725-729.
13. Losego, M.D., M.E. Grady, N.R. Sottos, D.G. Cahill, and P.V. Braun, *Effects of chemical bonding on heat transport across interfaces*. Nature Materials, 2012. **11**(6): p. 502-506.

14. Wang, R.Y., R.A. Segalman, and A. Majumdar, *Room temperature thermal conductance of alkanedithiol self-assembled monolayers*. Applied Physics Letters, 2006. **89**(17): p. 3.
15. Wang, Z.H., J.A. Carter, A. Lagutchev, Y.K. Koh, N.H. Seong, D.G. Cahill, and D.D. Dlott, *Ultrafast flash thermal conductance of molecular chains*. Science, 2007. **317**(5839): p. 787-790.
16. Segal, D., A. Nitzan, and P. Hanggi, *Thermal conductance through molecular wires*. Journal of Chemical Physics, 2003. **119**(13): p. 6840-6855.
17. Sadat, S., Y.-J. Chua, W. Lee, Y. Ganjeh, K. Kurabayashi, E. Meyhofer, and P. Reddy, *Room temperature picowatt-resolution calorimetry*. Applied Physics Letters, 2011. **99**(4).